Detection of slush on the Greenland Ice Sheet using Moderate Resolution Imaging Spectroradiometer (MODIS) satellite imagery

Viktor Wu

2020
Department of
Physical Geography and Ecosystem Science
Lund University
Sölvegatan 12
S-223 62 Lund
Sweden

Viktor Wu (2020)
Detection of slush on the Greenland Ice Sheet using Moderate Resolution Imaging Spectroradiometer (MODIS) satellite imagery
Förändringsanalys av slask på Grönlandsisen
Bachelor's degree thesis, 15 credits in *Physical Geography and Ecosystem Science*
Department of Physical Geography and Ecosystem Science, Lund University
Geological Survey of Denmark and Greenland

Level: Bachelor of Science (BSc)

Course duration: *March* 2020 until *June* 2020

Detection of slush on the Greenland Ice Sheet using Moderate Resolution Imaging Spectroradiometer (MODIS) satellite imagery

Viktor Wu

Bachelor thesis, 15 credits, in *Physical Geography and Ecosystem Science*

Per-Ola Olsson
Department of Physical Geography and Ecosystem Science

Baptiste Vandecrux
Geological Survey of Denmark and Greenland

Exam committee:
Ulrik Mårtensson
Fredrik Lagergren

Abstract

Sea Level Rise (SLR) is a growing global concern that is heavily influenced by a warming climate. Because of a potentially large added mass to the ocean through ice melt, the Greenland Ice Sheet (GrIS) plays an important role in the contribution to SLR. The presence of slush on Greenland is the result of melting processes and it can work as an indicator of surface mass balance (SMB) patterns on the ice sheet. This paper presents a detection of slush on the GrIS and the spatiotemporal evolution of slush during the study period 2000-2019. An upper limit of slush, known as the slush-line is also presented. A method is used which looks at spatial variability of albedo to detect slush on Moderate Resolution Imaging Spectroradiometer (MODIS) satellite imagery.

Classification of daily satellite imagery during the study period showed a presence of slush mainly during the melting season mid-May to September each year. During the study period, slush-extents and the elevation of the slush-line were fluctuating over the years. An exceptionally large presence of slush was detected during the summer of 2012. Greater areas of slush were found on the western areas of the ice sheet; particularly large areas of slush were detected in the southwest. Slush-extent and the elevation of the slush-line showed a generally positive correlation, where an increased slush-extent results in a higher slush-line elevation. This relationship was particularly strong in the western and southern areas, while a weaker relationship was found in the eastern and northern parts of the ice sheet. This pattern is potentially related to variations in complexity of the physical environment. General developments of slush-extents over the study period show an agreement with previous studies on mass balance and particularly agree with measured cumulative melt-day extents for each year.

Key words: slush, Greenland Ice Sheet (GrIS), surface mass balance (SMB), sea level rise (SLR), satellite imagery.

Table of Contents

1. Introduction

The future of the world's climate is uncertain and could impact all of the world and its inhabitants, potentially causing damage, taking lives and destroying ecosystems. Anthropogenic emissions of greenhouse gases have massively increased since 1850, contributing to a warming climate. During the last century, temperatures have increased and the Intergovernmental Panel on Climate Change (IPCC) Fifth Assessment Report (AR5) predicts that temperatures will further increase during the 21st century according to all assessed emission scenarios (IPCC 2014). The predicted scenarios include increased occurrence of extreme events, droughts, ocean acidification and glacial retreat among other destructible events. One potentially destructible effect of a warming climate is rising global sea levels, affecting low-lying coastal areas and their inhabitants. Over the period 1901–2010, global mean sea level rose by 0.19 ± 0.02 m. With warmer temperatures, the sea level is expected to further increase for centuries to come (IPCC 2014).

Nicholls et al. (2011) estimate a potential sea level rise (SLR) of 0.5 to 2 m based on a scenario of a 4 °C or greater increase in temperature by 2100. A mean global sea level rise of 0.5 m is estimated to result in the displacement of 70 million people assuming no measures of protections are taken (Nicholls et al. 2011). Furthermore, lower elevation coastal zones expect an increase in populations over the following decades (Neumann et al. 2015). The estimated predictions of SLR combined with an increased coastal population make global sea level rise an increasingly worrying threat.

Sea level rise due to an increased temperature happens partly due to thermal expansion of the water as it heats, but mainly due to an increased ocean mass (Stephens et al. 2020). This increased mass comes from a mass loss of ice, happening at glaciers, ice caps and ice sheets. The two great ice sheets, the Antarctic ice sheet and the Greenland Ice Sheet are therefore of massive importance with regards to global sea level rise.

1.1 Albedo and Slush

Slush is a resulting feature of the melting processes causing melt-water to move towards lower ends of melting areas where it saturates the snow. Slush is in this study defined as a snowpack that is saturated with water over its entire depth and lies on top of ice. A slush-line is described as a locator for the limit between slush covered surfaces and surfaces covered with ice or dry snow.

Slush, as well as other features like water, ice or dry snow can be identified by its spectral attributes like albedo. Albedo represents the ratio of reflected incoming solar radiation of a surface, and describes this with a number between 0 and 1. The value of albedo differs between ice, slush and snow. This is explained by their physical composition and the color of the surfaces. Snow has a very high albedo, being of white color and composed of air bubbles which contribute to the reflection of incoming radiation. Ice has a lower albedo, often with a darker surface because of accumulated darker material. Slush has an albedo in between the two, as it is similar to snow but saturated with water, which is more absorptive and allows light to penetrate deeper. Because of this relationship, areas that go from ice to dry snow, with slush in between, are likely to have a higher variability in albedo than more homogenous areas.

Surface albedo is used in several studies to estimate and describe mass loss and increased runoff (Hofer et al. 2017; Ryan et al. 2019). Ablation zones in particular are often investigated and determined with observations of albedo and its variability due to the known differences in spectral properties (Boggild et al. 2010; Ryan et al. 2019). Since net shortwave radiation has the main impact on surface melt, the role of albedo is important in describing energy exchange between surface and the atmosphere (van den Broeke et al. 2008).

1.2 Greenland Ice Sheet

The world's second largest ice body, the Greenland ice sheet (GrIS), has a volume corresponding to a sea level equivalent (SLE) of 7.4 m (Vaughan et al. 2013). This means that if the ice sheet would melt completely, global sea levels would rise by 7.4 m. Over the past 20 years, the ice sheet has undergone dramatic change and melt is evidently increasing across the ice sheet (Velicogna 2009; Ryan et al. 2019; Scambos et al. 2019). The 7 years of highest melt since 1978 have all occurred within the past 20 years (Scambos et al. 2019). This increase in melt has occurred along with changes in surface coverage and is related to a decrease in albedo associated with feedback loops (Box et al. 2012; Ryan et al. 2019). A consistent response of the GrIS to warmer temperatures make the ice sheet's contribution to global sea level rise a growing concern when considering future climate predictions. IMBIE Team (2020) predicts a further contribution of 0.07 to 0.13 m from the GrIS to global sea level rise by year 2100 if the climate changes according to the upper ends of the IPCC AR5 projections.

1.3 Aim

This study aims to describe the spatiotemporal evolution of the Greenland Ice Sheet over the period 2000–2019 with regards to presence of slush and the movement of the slush-line and slush elevation. The seasonal behavior of slush is studied both for the Greenland Ice Sheet and on a drainage basin level. Specific research questions are:

- Can slush be mapped with coarse resolution satellite data?
- When did the ice sheet experience the greatest extents of slush?
- Which parts of Greenland have the largest area of slush?
- How does slush-extent and the elevation of the slush-line relate to each other?
- What are the differences between the drainage basins?

Investigating the extent of slush as well as the movement of the slush-line is of interest as it describes the variations of mass balance on the ice sheet, which relate to the contribution to SLR. The spatiotemporal evolution of the extent of slush and the slush-line on the GrIS has the potential to outline changes in melt-rates and the responses of the ice sheet.

1.4 Background

Several studies present an increased mass loss and increased runoff on the GrIS (Velicogna 2009; Rignot 2011). A study by Ewert et al. (2012) estimates annual mass loss based on laser altimetry data, giving an SLE of 0.53 ± 0.06 mm yr$_{-1}$ when investigating two periods, September–November 2003 and February–March 2008. van den Broeke et al. (2016) investigated mass balance changes across the ice sheet and found that the accelerating melt occurring on the GrIS has a significant impact on global sea level rise. It was estimated that the average annual mass loss over the period 1991-2015 has an SLE averaging at

~0.47 ± 0.23 mm yr.1 with a peak contribution to SLR during the study period in 2012 when the estimated SLE reached 1.2 mm for that year. 2012 proved to be an exceptionally warm year of record melt both in terms of mass loss and reached elevations of melt (Nghiem et al. 2012). Bamber et al. (2018) compared several estimates of mass balance based on different techniques, focusing on the IPCC AR5 report and more recent studies than the IPCC report. With the studies and estimates from IPCC AR5, a weighted mean for mass balance was calculated. Over the period 1992–2016, results show a general increase in mass loss up until 2012 which shows the greatest mass loss. NSIDC presents a development in the total melt-day area during the study period where 2012 stands out. Here, high melt-extents and 6 other of the highest melt-years since 1978 are shown (Scambos et al. 2019). A bar chart of the melt-extents is shown in Figure A1.

The evident mass loss indicates an increased extent of slush, as more meltwater will be produced. Particularly warm and high melt-years like those of 2010 and 2012 are most likely also years of great slush-extents and elevations reached.

The melting season on Greenland is defined as the time during which melt is occurring on 5 % or more of the Ice Sheet surface. Three consecutive days have to be above the threshold for an individual day to count (Scambos et al. 2019)

Greuell and Knap (2000) studied the movement of the slush-line on a section of the Greenland Ice Sheet. Their method uses albedo grids derived from Advanced Very High Resolution Radiometer (AVHRR) images. Cloud-free images were used and albedo values were manually calculated according to the methods of Knap and Oerlemans (1996). The spatial resolution of the images is 1 x 1 km and the classification of slush was based on the spatial variability of the albedo grid cells. Within a 5x5 pixel window, slush is identified where albedo variability is reaching and exceeding a threshold of a standard deviation of 1.25 %. The study focuses on finding the transition in spatial variability of albedo that is associated with the slush-line, seeing slush-covered areas as a mosaic of mixed albedo values. Consequently, snow or ice-covered areas are considered as having a lower variability in albedo, more specifically under the threshold of a standard deviation of 1.25 %. The maximum slush-line during the study period 1990–1995 did almost not move at all but is still assumed to be subject to change with climatic variations. It was found that more melt resulted in higher slush-line elevations and slush located further inland. Lower melt resulted in lower elevations and makes sense with the assumed responses of the slush-line to climatic variations.

Since 2000, satellite-derived albedo from the NASA platform Moderate Resolution Imaging Spectroradiometer (MODIS) is available. The MOD10A1 Collection 6 product provides daily cloud-free surface albedo data. Some features of clouds like edges, shadows or condensation trails may still be included in some cases due to the similar spectral properties of clouds and the surface of brighter areas with clean snow. In order to reduce the presence of cloud features, statistics from an 11-day interval are calculated and a pixel is replaced by the 11-day mean value in case the variation of these daily albedo values is below a certain threshold (Box et al. 2017). Furthermore, the albedo grids with de-noising, gap filling and bias correction are validated. Box et al. (2017) describes the product and compares it to ground-truth albedo measurements from automatic weather stations from The Greenland Climate Network (GC-Net) and from The Programme for Monitoring of the Greenland Ice Sheet (PROMICE).

GC-Net automatic weather stations have monitored albedo since 1995, while PROMICE stations have been available since 2007. For each year, nearest albedo value from the satellite-derived data is compared with the value retrieved by the weather station. This is done at every station location. Comparing the de-noised satellite data with raw data, the de-noised satellite data shows a better agreement with the ground data.

2. Data and Methodology

2.1 Data

The MODIS MOD10A1 Collection 6 product providing satellite-derived albedo over Greenland is used. The albedo product is provided by Box et al. (2017). In addition to albedo, the dataset also includes elevation data, geographical coordinates and an ice mask to define the ice sheet. The grids consist of 5 km x 5 km pixels of an area covering all of Greenland where each pixel has an albedo value between 0 and 1. Ice mask values range between 0 and 2 where only pixels with a value of 1 are considered part of the ice sheet. Each pixel has an elevation in meters above sea-level and longitudes and latitudes given in degrees East and North. For regional analysis, drainage system boundaries for Greenland were used (Zwally 2012). The dataset containing drainage system boundaries was developed by the Goddard Ice Altimetry group at NASA.

2.2 Classification

Daily satellite-derived albedo grids from 2000 to 2019 over Greenland were used as the main input and were individually classified into three classes; slush, land and dry snow/bare ice. The classification was performed with a program written in Python which classifies each pixel of a satellite image based on its absolute value of albedo or its spatial variability of albedo.

In this study, a method similar to that of Greuell and Knap (2000) was used. Greuell and Knap (2000) use AVHRR satellite images with a spatial resolution of 1 x 1 km. They use a threshold value of a standard deviation of 1.25 % for the spatial variability in albedo, above which pixels are classified as slush. They use a 5x5 pixel window to determine the standard deviations of albedo. In this study, satellite imagery with a coarser spatial resolution is used, and a larger area is classified. Using the same threshold and window-size is therefore deemed inappropriate and would yield unrealistic results with regards to observed melt on Greenland (NSIDC 2019).

The window-size used in this study for calculating variability is 3x3 pixels and the threshold value used for spatial variability in albedo is a standard deviation of 5 %. This value is chosen based on field evidence of a slush-line location. On the 12th of July 2012 at the automatic weather station KAN_U in western Greenland, the upper limit of slush was observed at the station location. Using this information as ground-truth, a threshold value was defined. The value was retrieved through attempted classifications combined with visual observations of the slush-line. Finally, the threshold value chosen was the value which for the satellite image of 12th of July 2012 generates a slush-line at the location of the KAN_U automatic weather station. The weather station location and albedo scenario during the 12th of July 2012 as well as the classified image is visualized in Figure 1.
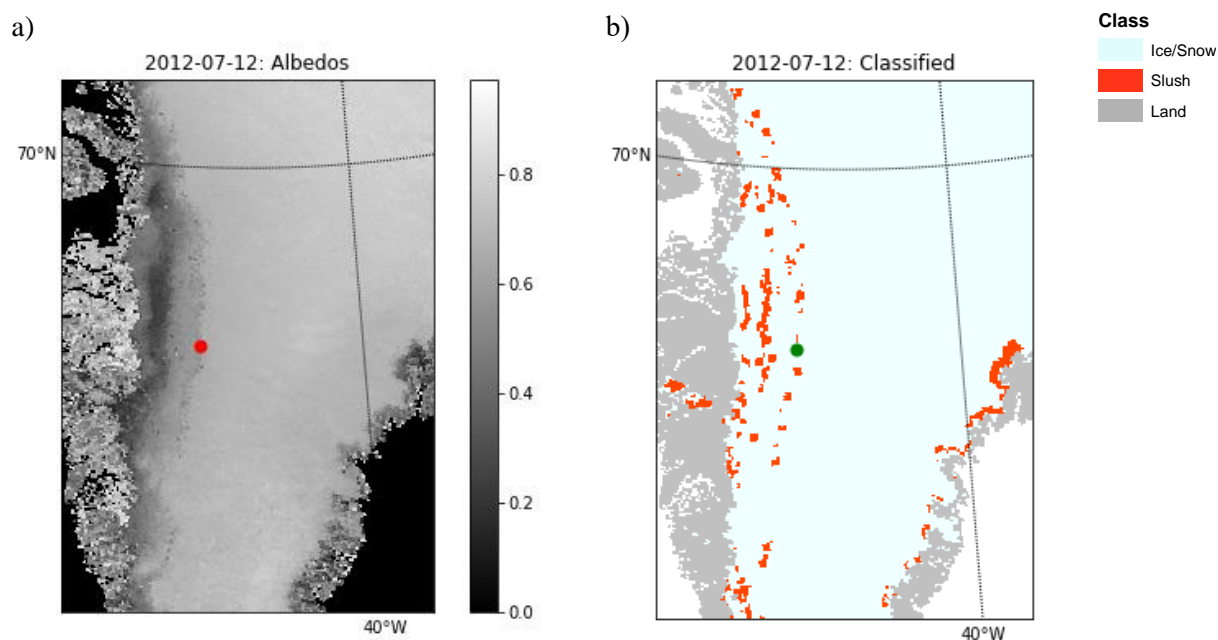
a)

b)

Figure 1:Area surrounding the KAN_U automatic weather station in Southwestern GrIS. Green and red dots mark the location of the weather station. Figure 1a shows the MODIS satellite-derived albedo grids from Box et al. (2017). Pixels with albedo-values range between 0 and 1. Figure 1b shows classified grids where pixels are colored by class. Slush is displayed in red, bare ice or dry snow is light blue and land is gray.

In addition to the conditions regarding spatial variability of albedo, two other conditions have to be fulfilled in order for pixels to be classified as slush. Slush is defined as lying on top of ice and should not be mistakenly recognized in land areas of higher spatial variability in albedo. A high spatial variability of albedo in land areas can be seen in Figure 1. Therefore, one of the criteria a pixel must meet in order to be classified as slush is that it must have an ice mask value of 1, or in other words be on top of the ice. The final condition is that a pixel according to the spatial variability in albedo should be classified as slush less than 2800 times over the study period, which equates to an average of 140 days per year. Pixels classified more than 2800 times are not considered slush pixels as slush can only exist during the melting season which usually runs from mid-May to September, corresponding to less than 2800 days during the 20 years long study period (Scambos et al. 2019).

The classification needs to consider the amount of cumulative slush-days as it otherwise misclassifies pixels as slush during the winter. Generally, these errors are attributed to a spatial variability caused by neighboring cells of land or water, which unsurprisingly results in large differences in albedo values. The variability in albedo intended to describe slush refers to the variability within what is on the ice, and not between pixels of ice *and* land. An example of consistently misclassified slush pixels due to neighboring cells of land or water is shown in Figure 2, where slush pixels which are identified nearly every day of the study period coincide with the locations where ice meets land or even water.

a)

Cumulative slush-days

b)

2019-10-29

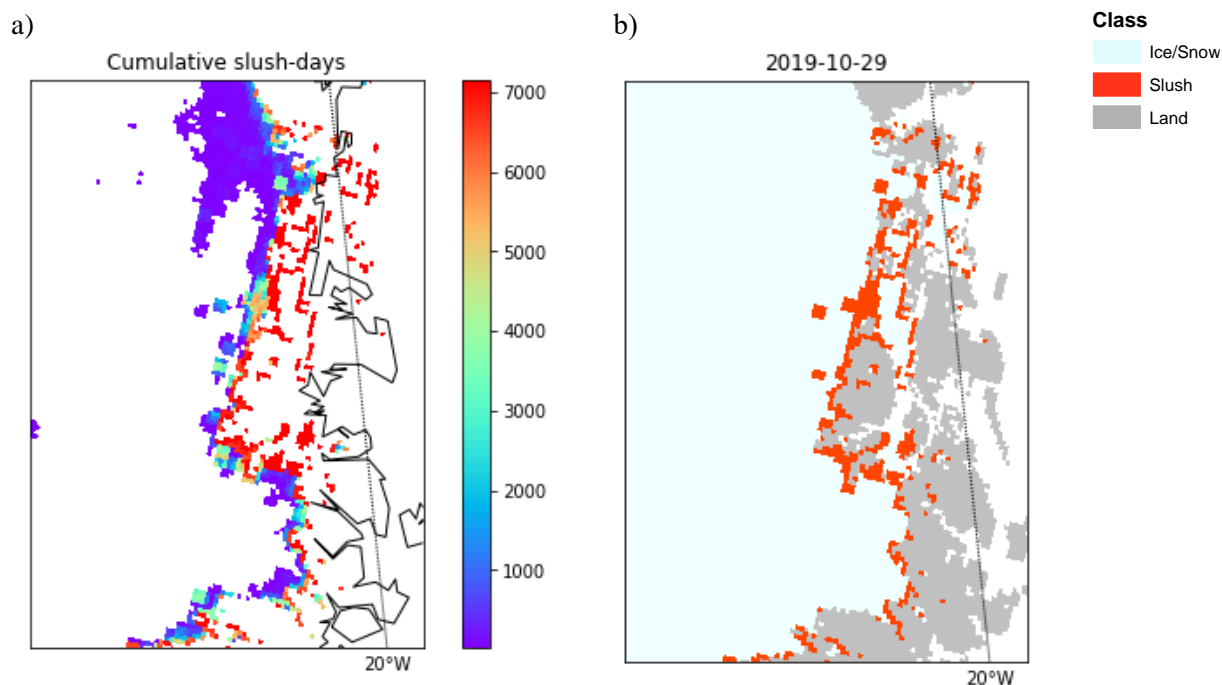**Class**

Ice/Snow

Slush

Land

Figure 2: Classified slush on a section of northeastern GrIS. Figure 2a shows cumulative slush-days during the study period, where colors towards the red end of the spectrum indicate a large amount of days classified as slush. Figure 2b shows a classification where no limit in cumulative slush-days has been set. Slush-pixels are shown in red. The classified satellite image is from 29th of October 2019.

2.3 Analysis

The resulting maps were plotted in Python for a visualization of the spatial distribution of slush. Each class, slush, ice/dry snow or land was displayed in different colors and maps were made for analysis of the entire ice sheet as well as smaller individual areas or drainage systems.

Slush-pixels and their elevations were counted in order to quantitatively analyze the temporal evolution of slush on the GrIS. Pixels were divided into drainage systems by finding their location within polygons for each drainage system, which were created using data with the geographical borders of each drainage system (Zwally et al. 2012). This allowed for slush-extents to be calculated and slush-line elevations to be estimated for each day and each drainage system. Plots were made displaying slush-extents and slush-line elevations over the study period.

Slush-pixels were counted, and their elevation data was retrieved. To determine the elevation of the slush-line, a maximum value of these elevations was not chosen, but rather a 90th percentile of the distributed elevations. In the distribution of elevation values, some elevations towards the extremes are identified as outliers. This is because various errors can cause a spatial variability in albedo that is not attributed to slush. An upper limit of slush is therefore in this study represented by the 90th percentile of the distributed elevations in order to disregard outliers.

Counting slush-pixels was also the method for making a cumulative slush-day map, which is used to filter out the slush-pixels that are incorrectly classified as slush year-round. The cumulative slush-day map,

when displaying slush-day values below the threshold of 2800 is also used to identify so-called hotspots or slush prone areas.

A slope map was produced using the elevation data to analyze hotspots and their occurrence on slopes. From the elevation data each cell is programmed to calculate the slopes to its 8 surrounding cells. Here, slope is calculated as the difference in elevation between two cells over the distance between the two centers of the cells. An absolute value of the change in elevation is calculated for each surrounding cell and divided over the distance between cells. The steepest slope is then chosen as the slope value for a cell. Both downhill and uphill slopes are considered. This method is similar to that of Sharpnack and Akin (1969).

In order to compare and describe the sensitivity of our classification, a threshold comparison was made. Albedo grids from 12th of July 2012 were classified three times, starting with a threshold of a standard deviation of 4 % and increasing with one percentage point each time. Three larger regions were plotted and displayed in map-format for a visual comparison. Additionally, the change in slush-pixels per changed threshold value was calculated for each drainage system in order to make a quantitative comparison.

Ground-truth data regarding slush is limited and it is therefore difficult to validate a method attempting to identify all slush on the GrIS. In order to give a visual analysis on the accuracy of the classification a satellite image was compared with a classified image. A satellite image from 30th of August 2016 visualizing Normalized Difference Water Index (NDWI) was collected from the EO Browser at Sentinel Hub (Sinergise Ltd. 2020). The image is from the Sentinel-2 L1C dataset and is of 10 x 10 m spatial resolution. The image was manually interpreted, and a figure was made which highlights areas considered slush, bare ice and dry snow. This image was compared with a classified image of the corresponding area and day.

3. Results

3.1 Slush on the Greenland Ice Sheet

The classification presents a seasonal variation in slush where the presence of slush coincides with the melting season on Greenland. Colder months (November to May) show little to no slush pixels across the entire ice sheet over the entire study period.

Slush is generally observed at the edges of the ice sheet, towards the ends of the melting areas. Further, a peak slush-extent is typically observed in mid-August. Figure 3 shows the seasonal development of slush and its presence in the margins of the ice sheet and particularly on the western side of the ice sheet. For all displayed years, June and October display far less slush than the other three months closer to the peak of the melting season. Generally, the 1st of August and September tend to display the greatest slush-extents. The spatial distribution is more clearly displayed in Figure 4, which shows classified images from the particularly high melt year 2012.
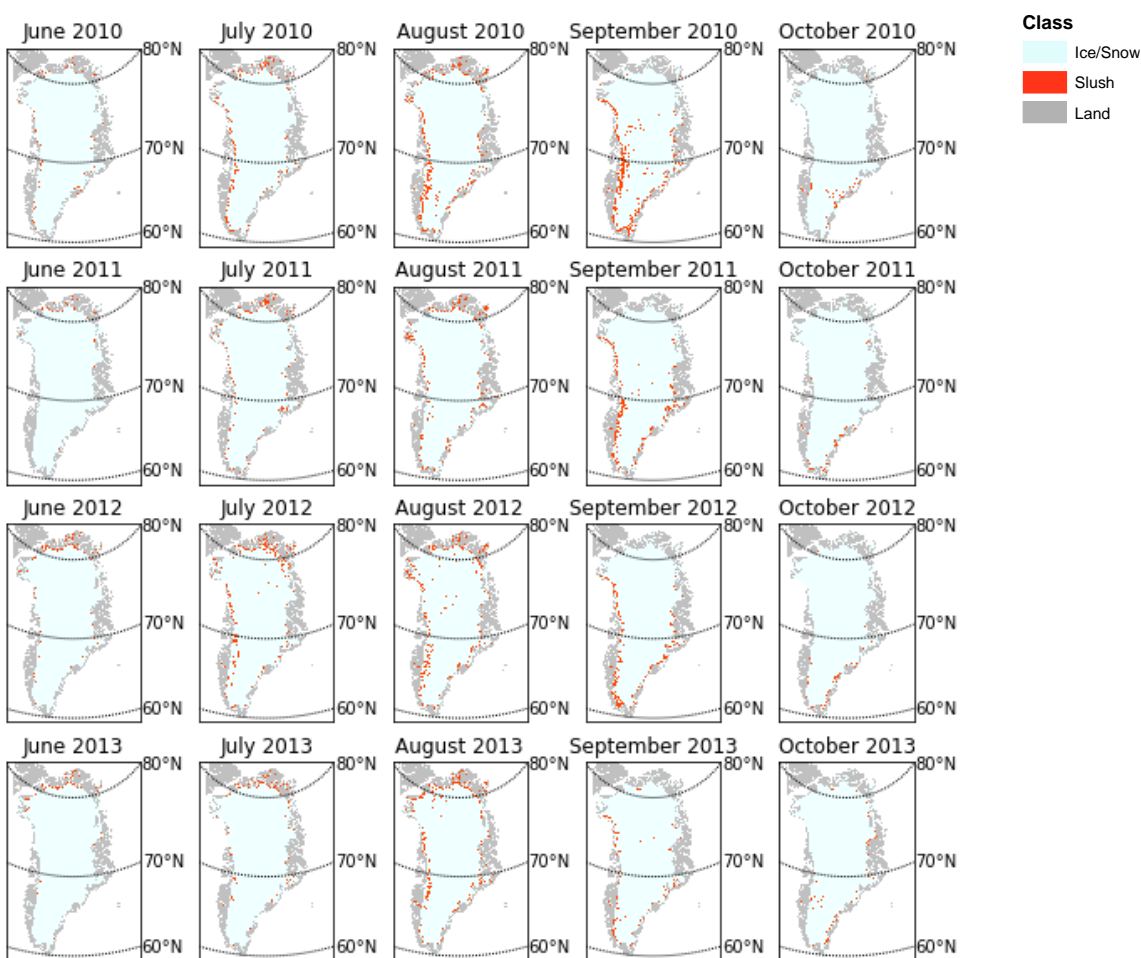
Figure 3: Classified images for the 1st of each month in June-October 2010-2013. Slush is displayed in red, bare ice/dry snow as light blue and land is gray.
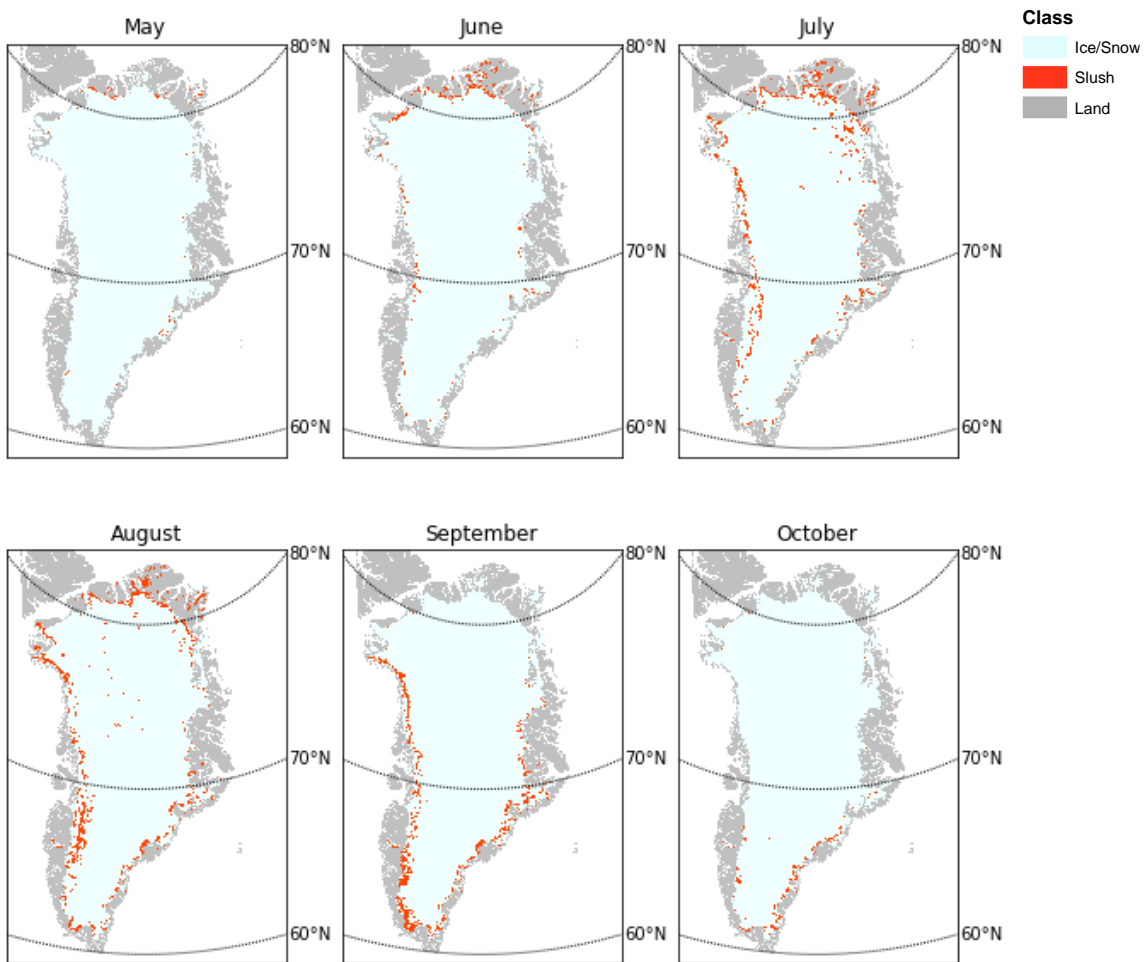
Figure 4: Classified images for the 1st of each month in June-October, 2012.

Furthermore, plots based on maximum slush-extent days of each year (Figure 5) visualize the changes quantitatively and allow for a more detailed display. Over the Greenland Ice Sheet, a large peak in slush-extent is observed in 2012 with fluctuations before and after. Slush-line elevations are generally increasing and decreasing simultaneously with the slush-extent but at different rates. The elevation of the slush-line appears to reach as high as 2100 m three times during the study period. The large peak, representing the greatest slush-extent during the study period was detected on 12th of August 2012.

A median slush-extent of 587 350 km² was calculated for the maximum slush-extent days during the study period on the GrIS. For the slush-line elevation, a median of 1888 m was calculated. The relationship between slush-extents and slush-line elevations on the ice sheet has a Pearson correlation coefficient of 0.266, indicating that the relationship is positive but not particularly strong.
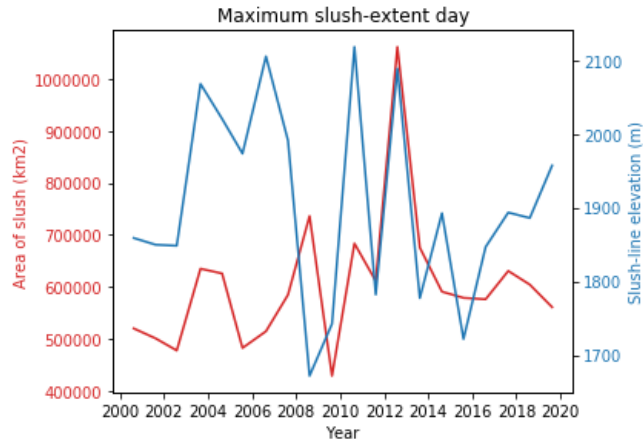
Figure 5: Slush-extent (left axis) and Slush-line elevation (right axis) over the study period. Slush-line elevation is given as the 90th percentile of the elevations on which slush is detected. Values represent the day of each year that has the greatest slush-extent.

3.2 Slush on individual drainage systems

Table 1: Statistical measures of slush-extent and the slush-line elevation from the days of maximum slush-extent each year of the study period 2000-2019 for the drainage systems of Greenland (see Figure A2). A Pearson correlation coefficient is shown to describe the relationship between slush-extent and the slush-line elevation. Mean, median and standard deviation values are shown for slush-extent and slush-line elevation. Values highlighted in yellow are the highest slush-extent mean and median values.

	Slush-extent (km2)			Slush-line elevation (m)			Correlation
Drainage system	Mean	Median	St. dev. %	Mean	Median	St. dev. %	Coefficient
GrIS	603526	587350	0.011	1904	1888	0.003	0.266
1.1	34550	28225	0.050	1504	1373	0.014	0.140
1.2	17850	16213	0.048	1518	1378	0.024	0.001
1.3	14951	12713	0.049	1390	1293	0.027	0.132
1.4	11386	9013	0.044	1031	1160	0.019	0.639
2.1	26928	21213	0.040	2316	2495	0.012	-0.159
2.2	4423	3938	0.032	1879	1901	0.005	0.688
3.1	17883	17613	0.018	2220	2166	0.003	-0.097
3.2	20471	20663	0.011	2412	2407	0.001	0.271
3.3	17521	15838	0.013	2256	2266	0.002	0.049
4.1	17741	17975	0.016	2294	2276	0.003	0.140
4.2	11341	9913	0.024	1455	1273	0.012	0.718
4.3	5681	4775	0.025	1895	1854	0.006	0.631
5.0	32073	29763	0.019	1830	1778	0.006	0.115
6.1	23353	19988	0.035	1869	1813	0.006	0.446
6.2	130244	123700	0.028	1706	1689	0.005	0.675
7.1	25760	22825	0.026	1610	1565	0.006	0.821
7.2	37981	34113	0.031	1771	1776	0.003	0.489
8.1	73410	61725	0.024	1723	1475	0.013	0.472
8.2	31736	31363	0.019	1269	1214	0.007	0.132

Individual drainage systems show similar behavior to that of the entire ice sheet, with fluctuations generally going in the same direction for slush-extent and slush-line elevation, indicating a positive relationship where an increased slush-extent also leads to an increased slush-line elevation (Figure 6). A positive correlation coefficient was calculated for all drainage systems except 2.1 and 3.1, which show negative coefficients (Table 1). For some drainage systems, there is a stronger agreement between the plotted lines. Drainage systems located on the eastern and northern side of the ice sheet tend to show less of an agreement between the two lines. A relationship between slush-extent and slush-line elevation appears to be more consistent in the western areas (Figures 6c and 6d) as opposed to the eastern side (Figures 6a and 6b) of the ice sheet. Table 1 indicates stronger correlation-coefficients for drainage systems located on the southern or western parts of the ice sheet, compared to the eastern and northern parts. The geographical locations of the drainage systems can be found in Figure A2.
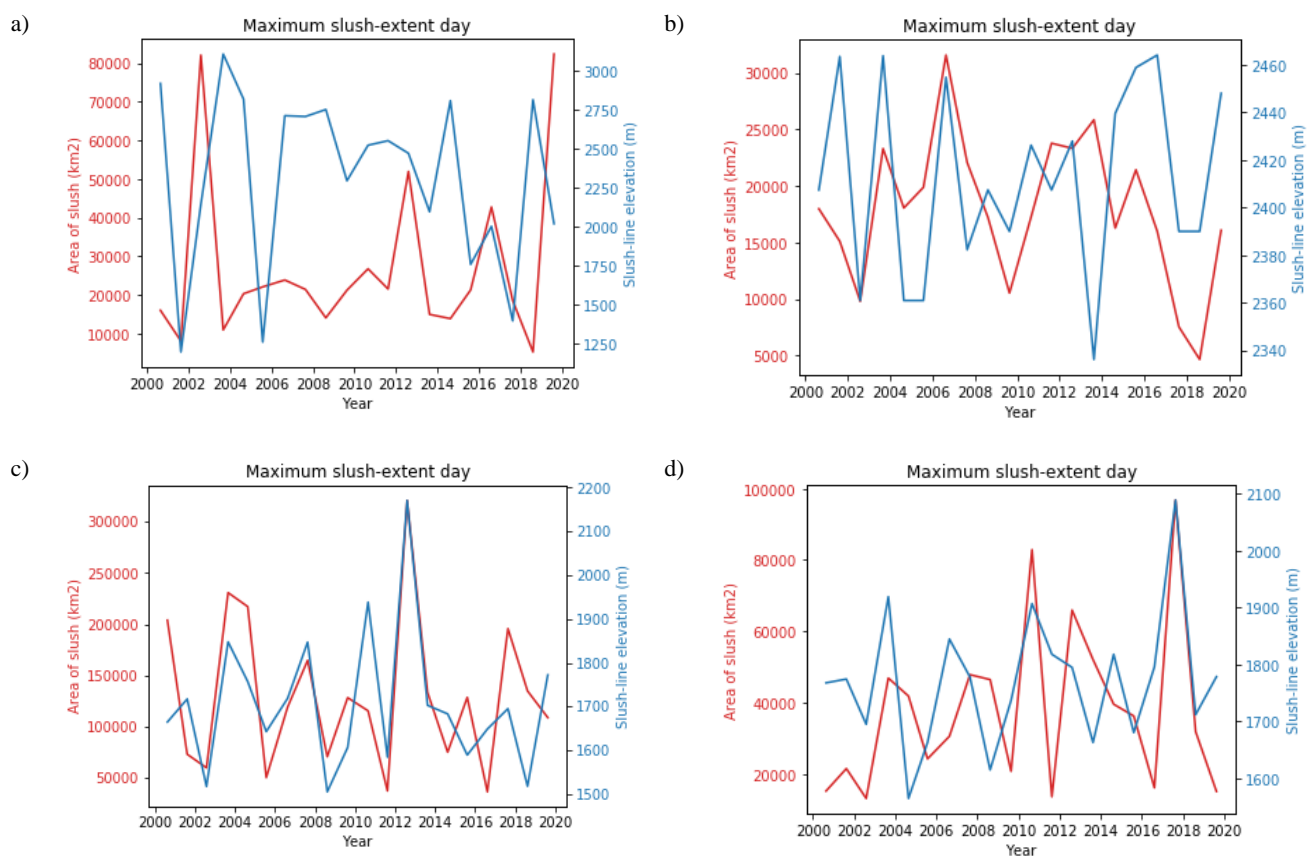

Figure 6: Slush-extent in km2 and slush-line elevation in meters above sea-level during the study period 2000-2019 for Drainage system 2.1 (Fig. 6a), Drainage system 3.1 (Fig. 6b), Drainage system 6.2 (Fig. 6c) and Drainage system 7.2 (Fig 6d). Values represent days of maximum slush-extent. Slush-line elevation is given as the 90th percentile of the elevations on which slush is detected.

Results from Table 1 show that Drainage system 6.2 has had the greatest amount of slush during the study period, averaging an area of 130 244 km$_2$ covered by slush on the days with the greatest extent of slush. The strongest correlation between slush-extent and slush-line elevation is found in drainage system 7.1 on western Greenland.

3.3 Slush-hotspots

Throughout the study period slush is detected mainly in the margins of the ice sheet. Plotted cumulative slush-days indicate a dominant presence of slush especially in the western areas of the ice sheet. In figure 7, purple pixels corresponding to 500 days of slush or less during the study period are found further inland compared to lighter blue or green which are found further down towards the margins of the ice sheet. Green areas indicate slush classified an average of 75 days per year which corresponds to a solid recurrence for most melting seasons. In western areas generally and southwestern especially, the width of slush-areas is larger than those in other areas of the ice sheet.
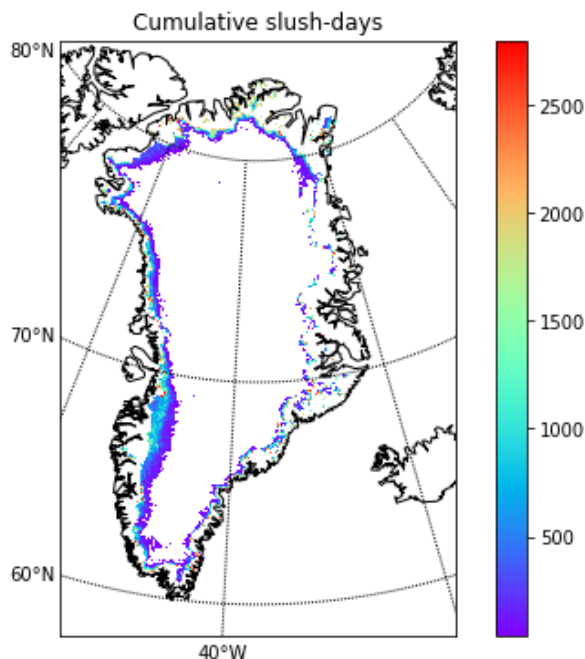

Figure 7: Cumulative slush-days over the study period 2000-2019. Values range from 20 to 2800 days.

Slush-hotspots and areas prone to slush creation were found through visual analysis and comparison of mapped cumulative slush-days with elevation-derived slope values. Results show slush-creation most often happening on lower slope-gradients (see Figure 8a), indicating that generally slush is found in flatter areas. Figure 8b indicates that most slopes present on the ice sheet also are of a smaller gradient. However, some pixels have a slope-gradient of 0.05 or higher, these are slope-gradients on which slush pixels very rarely are detected.
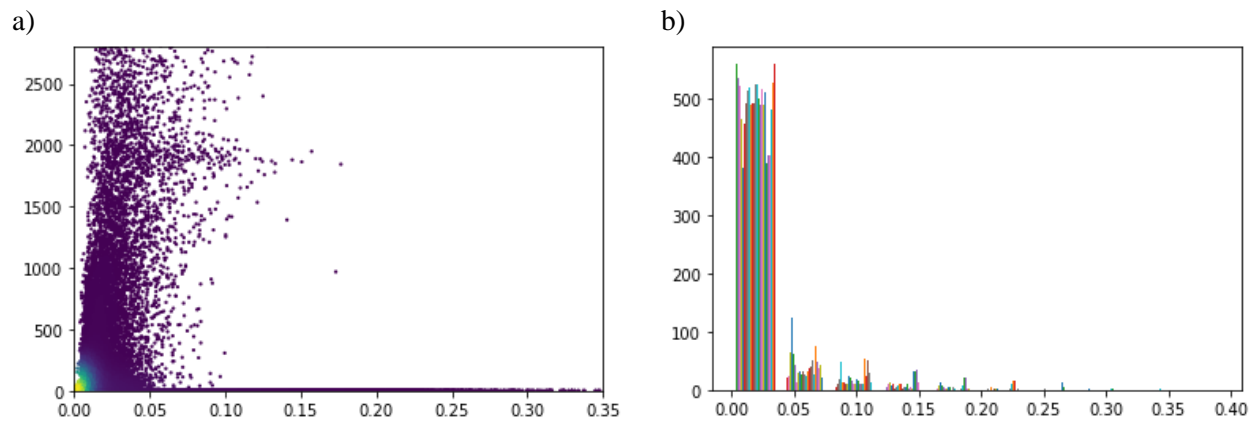
a)

b)

Figure 8: Slush-pixels and slope-pixels plotted over slope gradients. Figure 8a shows cumulative slush-days on the y-axis and slope-gradients on the x-axis. Brighter colors indicate a higher point density. Figure 8b is a histogram of slope-gradients on the ice sheet. The y-axis is the count of cells and the x-axis shows the slope-gradient.

A distribution of slope-gradients was found where drainage system 7.1 has the lowest slope-gradients and lowest standard deviation within these. The greatest slope-gradients and standard deviations were found in drainage system 3.2.

Table 2: Statistical measures of slope-gradients in different drainage systems. Slope values are derived from a Digital Elevation Map provided by Box et al. (2017)

	Slope-gradients across the drainage systems		
Drainage system	Mean	Median	St.dev
1.1	0.009	0.005	0.014
1.2	0.011	0.005	0.015
1.3	0.012	0.006	0.015
1.4	0.013	0.008	0.011
2.1	0.006	0.003	0.010
2.2	0.018	0.007	0.026
3.1	0.021	0.007	0.034
3.2	0.056	0.045	0.042
3.3	0.016	0.009	0.019
4.1	0.028	0.016	0.028
4.2	0.014	0.008	0.015
4.3	0.014	0.006	0.019
5.0	0.026	0.017	0.025
6.1	0.011	0.008	0.010
6.2	0.009	0.006	0.009
7.1	0.005	0.004	0.004
7.2	0.010	0.004	0.019
8.1	0.008	0.005	0.009
8.2	0.025	0.023	0.020

3.4 Preliminary sensitivity analysis

The visual comparison of slush classified with different thresholds for three large areas of Greenland can be seen in Figure 9. Three different thresholds of a spatial variability in albedo were tested. A standard deviation of 4, 5 and 6 % were used to classify the same image. Slush-pixels on the images indicate a higher sensitivity to threshold values in southwestern Greenland, where an increased threshold value seems to cause a greater decrease in slush-pixels compared to other areas. Quantitative comparisons show a similar pattern (Figure 10). Drainage basin 6.2 (where KAN_U AWS is found) and 6.1, both in southwestern Greenland show the greatest sensitivity to a changed threshold value.
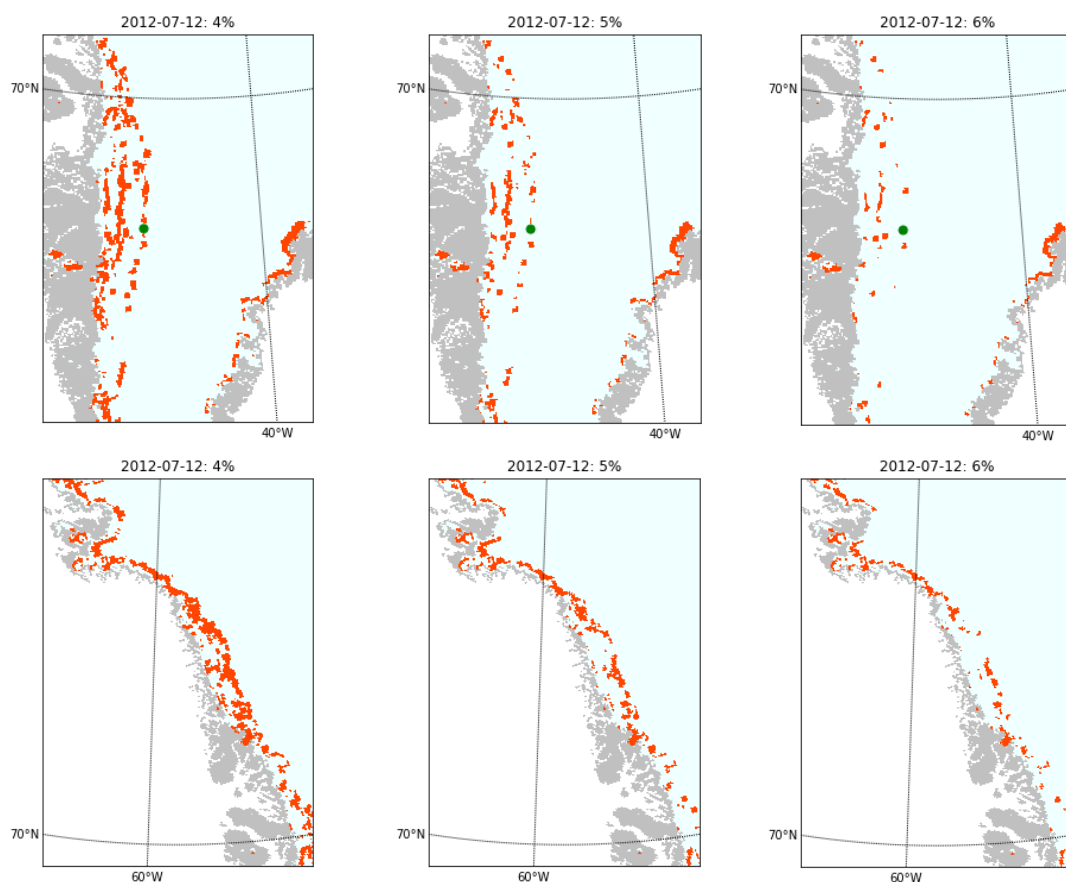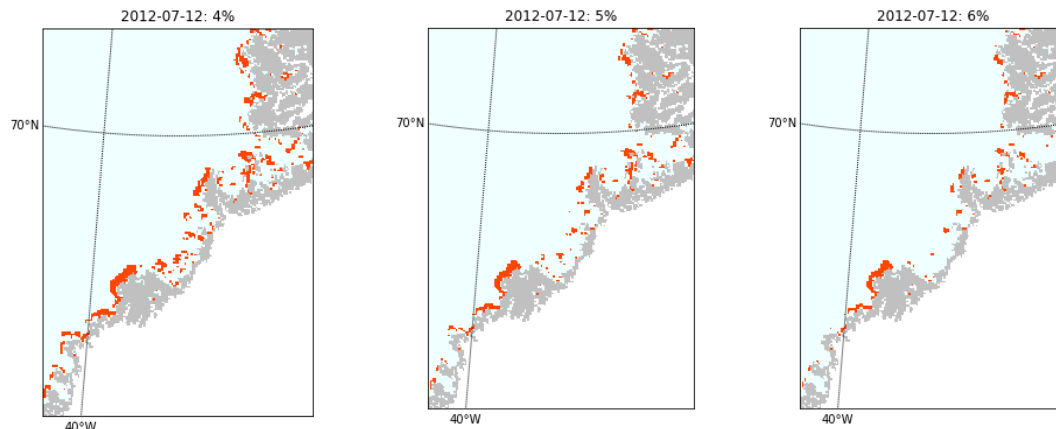
Figure 9: Maps from three areas classified with three different threshold-values. Panels on the left show a classification with a threshold of a standard deviation of 4 %, middle panels use 5 % and panels on the right have a threshold of 6 %.
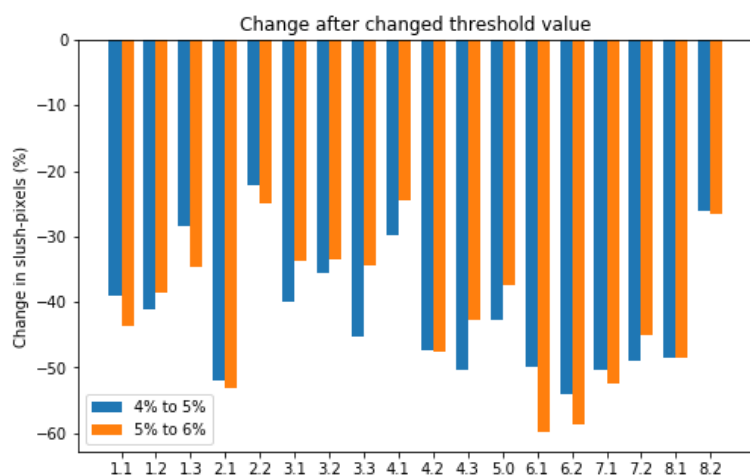

Figure 10: Relative changes in number of slush-pixels for each drainage system and changed threshold value.

3.5 Visual validation

The Sentinel-2 satellite image from 30th of August 2016, visualized as NDWI allowed for a manual interpretation to be made of the high-resolution image. Figure 11a displays a section of western Greenland, in drainage system 7.2. The area was interpreted to have some areas of bare ice in the very margins of the ice sheet, further inland they transition to areas of slush and in the north-east of the visualized area, a larger area of dry snow is found. Figure 11b shows the same area and the same day, classified according to the methodology of this study.

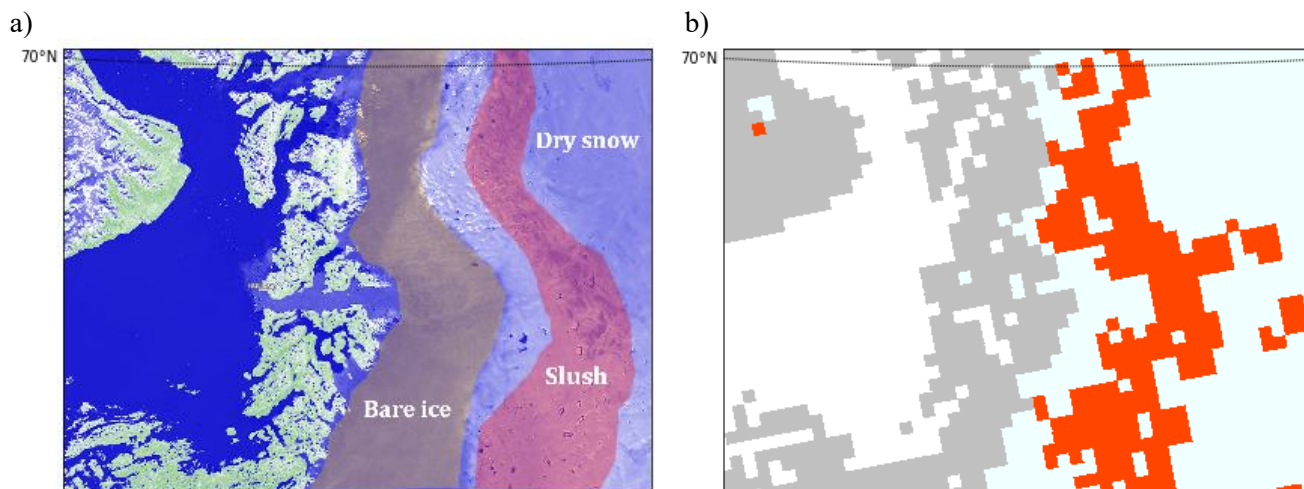a)   b)

Figure 11: Visually interpreted satellite image used for validation and a classified satellite image from the same area. Figure 11a shows areas of bare ice, slush and dry snow as they were interpreted. Figure 11b shows the same area, classified with the methodology of the study. Slush is depicted in red, bare ice/dry snow as light blue, and land as gray. Both images represent the conditions on an area of western GrIS on 30th of August 2016.

4. Discussion

4.1 Spatial and temporal evolution

Classified images of the Greenland Ice Sheet are showing both a spatial and temporal pattern in slush that in general agrees with expectations. The maps show a distribution where slush is present in the melting zones at the margins of the GrIS, which makes sense since slush is created through saturation of snow by melt-water. The seasonal variations also seem reasonable, where days during the winter months show no noticeable amount of slush. Because of the temperatures on Greenland during the winter season, melt is not realistic on the ice sheet and therefore no slush should be detected during that time. Despite occasional minor melt-events during April, September or October, the melting season typically runs from mid-May to September reaching a peak in July (Scambos et al. 2019)

The results show a presence of slush during the entire melting season with a maximum slush-extent typically occurring in mid-August. A consistent supply of meltwater to slush-areas will cause slush-extents to increase, which naturally results in slush-extents to peak later than the peak of the melting season. Slush-extents will only increase up until the point where refreezing starts to occur. Naturally, towards the end of the melting season some areas will still experience melt while others refreeze. Consequently, slush-creation will start to decrease some time before the melting season is over. Therefore, the day of maximum slush-extent in a year occurs towards the end of the melting season but not during the very last days.

The results show that the largest slush-extent in the studied period (2000–2019) occurred on the 12th of August 2012. This peak corresponds with information proving 2012 to be a year of exceptionally high melt-rates which consequently would result in a large extent of slush-areas. Several studies on the SMB

and runoff on the ice sheet as well as recorded data indicate that 2012 clearly experienced the highest melt during the study period (Nghiem et al. 2012; Mikkelsen et al. 2016; Scambos et al. 2019).

Studies on surface mass balance do not show a clear direction in which the mass balance is going over the entire study period. It is clear that the GrIS is losing mass, and although continuously negative - there are fluctuations in the mass balance over our study period. Generally, mass loss increases up until 2012 when it reaches a peak (van den Broeke et al. 2016; IMBIE Team 2020). The development of slush-extent from our classification seems reasonable based on the findings from previous studies. General fluctuations are seen here as well with a large peak in 2012.

Comparing the development of slush-extent on the entire ice sheet and the total melt-day area finds a good agreement. Figure 12 shows plotted values for slush-extent derived from this study and total melt-day area estimated by NSIDC (Scambos et al. 2019). The extent of slush detected in our study agree rather well with the cumulative melt-extents ($r_2 = 0.63$). Although not always of the same magnitude, the development from year to year seems to be similar. In most cases, an increased melt-day area also gives an increased slush-extent and vice versa.
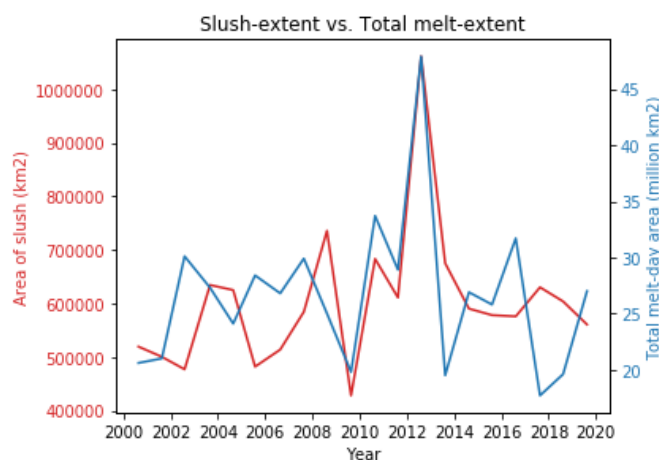

Figure 12: Yearly maximum slush-extent in km2 (left axis) plotted with cumulative melt extent in million km2 (right axis) over the study period 2000-2019.

4.1.1 Slush-hotspots

It is clear that a larger widespread area where slush is consistently detected is found on the southwestern part of the ice sheet (Figure 3, 4 and 7 and Table 1). This section of the ice sheet shows slush creation towards the margins of the ice sheet, occasionally moving inland under particularly high melt conditions. Some northwestern and northern areas also show extensive areas of slush-hotspots. The areas which show widespread and consistent slush-creation are also areas of generally homogenous topography and low slope gradients. Finding these areas as slush-hotspots is logical considering the physical behavior of melt-water and conditions required for slush-creation. Eastern areas show much smaller extents of slush along the margins of the ice sheet.

Looking at an elevation map of Greenland (Figure 13) it is possible to visualize how and where slush is created, as a result of melt-water moving down the drainage basins. With the elevation-derived slopes plotted against its cumulative slush-days (Figure 8), it is hard to see specifically how slopes relate to the amount of slush-days. However, it is seen that generally slush occurs in flatter areas, and often next to steeper slopes. This is logical as slush would be likely to move or runoff if it were on a steep slope. The coarse resolution of the satellite data is likely to produce gentler slopes and will naturally flatten out some steep slopes due to the long distance between the centers of two cells. There are still some steeper slope-gradients that have been derived from the elevation data. Slush is not found on these slopes, indicating that slush is likely to be created on flatter surfaces.
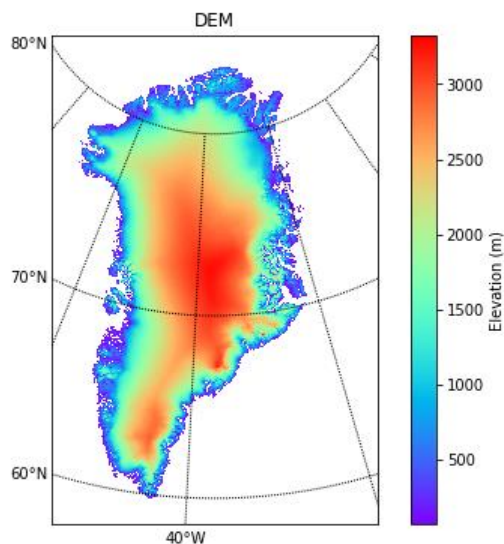

Figure 13: Digital Elevation Map over GrIS displaying elevation in meters above sea-level. Elevation data is included in the MODIS albedo product from Box et al. (2017)

Changes in slush-extents and the elevation of the slush-line can be seen in Figures 5 and 6. A comparison between the two often shows them going in the same direction, which is also indicated by the positive coefficient values found in Table 1. This shows a relationship where an increased slush-extent results in higher elevations reached by the slush-line. This is also logical considering the behavior of slush and slush-creation. A greater extent of slush, associated with higher melt-rates is more likely to reach higher elevations as the slush-areas expand under warmer conditions. Since slush-creation occurs at the lower ends of melting areas, an expansion of slush-areas would mean that more slush is created in the inland-direction, which also corresponds to higher elevations (see Figure 13). The higher melt-rates also cause melting to occur at higher elevations, supplying more melt-water and potentially saturating snow at higher elevations (Nghiem et al. 2012).

Although slush-extents and slush-line elevation generally have a positive correlation, they are often of different strength and most of the time, there is a clear difference between the plotted lines. This difference indicates that the slush-extent and slush-line elevation is not necessarily a linear function of melt. The varying correlations between slush-extent and slush-line elevations can be described as divided between certain types of drainage systems.

4.2 Slush-extent and slush-line elevation

Drainage systems in the western areas of the ice sheet, specifically drainage systems 6.1, 6.2, 7.1, 7.2 and 8.1 all show a moderate to good agreement between the development of slush-extent and of slush-line elevations. In addition to these, the southern drainage systems of 4.2 and 4.3 also seem to show a good relationship. Table 1 displays correlation values for these drainage systems ranging between 0.446 and 0.821. These drainage basins are also characterized by a more homogenous environment, and this is believed to be what contributes to better correlation coefficients. As opposed to eastern areas of Greenland, these areas have gentler slopes, larger drainage systems and less complex topography. Table 2 shows that the western and southern drainage systems in general have gentler slopes and less of a variation in slopes. One exception in this area is drainage system 5.0 which has steeper slopes and a greater variation in slope-gradients. However, drainage system 5.0 also shows a weak correlation between slush-extent and slush-line elevation. Along with this, it is evident both in our classification and in satellite images that a slush-line is more clearly identifiable on the western parts of the ice sheet, while the eastern parts show more of a chaotic environment and distribution of slush.

The northern drainage systems do not seem to follow the same pattern. Although they have relatively low slope-gradients, they produce weak coefficients of correlation. A comparison in the north shows that drainage system 1.4 has the steepest slopes, yet it has a considerably stronger coefficient of correlation. The fact that these drainage systems are not following a similar pattern, and generally produce very low coefficients of correlation, might be due to the classification being adapted to a location in the southwest. A threshold was set to produce results that agree with a ground-truth point in drainage system 6.2, which may not agree with the reality in northern drainage systems, but perhaps agree better with drainage systems that are closer, or of more similar climate.

There are a couple of reasons for the discrepancy between development of slush-extent and slush-line elevation on the eastern areas of Greenland. The main reason is the more spatially heterogeneous environment and topography of eastern areas relative to western. A chaotic environment of steep slopes and mountains makes it difficult for a slush-line to develop and to migrate gradually on to higher or lower elevations. Instead, it could go from one plateau to another depending on what the complex environment allows. This can create a disproportionate change in slush-line elevation compared to a more gradual change of slush-extent. Additionally, slush-areas representing the upper limits can be scattered on both high and low elevations, making a 90th percentile of slush-elevations less representative of the actual slush-line elevation.

A pattern where a larger homogeneity gives a better correlation coefficient for the drainage systems is seen in Table 2 and Table 1. In most cases a drainage system with a low mean slope-gradient and standard deviation also has a good correlation coefficient. This supports the theory that a slush-line cannot migrate at the same rate as the extent of slush and that the relationship between the two is therefore not consistent.

Additionally, there is a big difference between the amount of slush generated on the western and eastern areas of the ice sheet. Slush-extents on the western and southern parts of Greenland reach a total that is double the extents on the eastern and northern parts (Table 1). The considerably smaller amount of slush

detected in the eastern drainage basins make outliers or local variabilities not attributed to slush play a bigger role in estimating averages - both in slush-extent and slush-line elevation. Essentially, the eastern drainage systems have a smaller sample size as they contain fewer slush-pixels. This is one of the contributors to the differences and inability to find a relationship between the development of slush-extent and slush-line elevation.

Another reason could be that the discrepancies are caused or enhanced by errors. This is something that the more complex environment could contribute to. Presence of mountains and crevasses is likely to be higher in the east, which would affect the spatial variability of albedo. Another reason could be that eastern areas have a greater cloud cover during the summer months, increasing the risk of errors attributed to cloud-features (Lacour et al. 2018).

Describing a relationship between slush-extent and the elevation of a slush-line makes more sense where there is a clear slush-line. Western areas have less complex environments and often show a clear pattern with bare ice towards the margin of the ice sheet which transitions to an area of slush which further transitions to an area of dry snow at the location of a slush-line (Figures 1 and 11). This type of pattern is found on large areas of a more gentle and consistent slope across hundreds of kilometers. In these western areas, it seems that the slush-extent and the slush-line elevation relate to each other in a consistent way. An increased extent of slush areas results in an inland, and therefore upward movement of the slush-line.

The consistent behavior and patterns of slush along with the fact that western drainage systems are far more prone to slush-creation make them the most suitable for study and most representable for the evolution of slush over time.

4.3 Current limitations and future work

4.3.1 Data
Since the classification is based on MODIS satellite-derived albedo grids of 5x5 km resolution, this is also the resolution of the classification. 5x5 km is a relatively large area and slush could in reality be present in an area smaller than that. This makes it difficult to perform more detailed investigations. An example of the resolution being limiting is when choosing the threshold value. This was made based on the knowledge of slush being present at a very specific location, however because of the resolution of the grids - the presumably accurately chosen threshold value yields a slush-line at the station location but with an uncertainty of ± 5 km. In comparison to Greuell and Knap (2000), this study is unable to identify smaller areas of slush. It also requires a spatial variability in albedo caused by slush to cover an area 9 times higher (225 km_2) than that of Greuell and Knap (2000) (25 km_2).

The spatial resolution also plays a major role in the calculations of slope-gradients. Since the calculations are based on the difference in elevation between cells divided by the distance between the two, the coarse resolution will contribute to a relatively flat gradient. Steep slopes are likely to be existent within a 5x5 km area, but these are not recognized using satellite data of coarse spatial resolution. Although cloud-features in the images are reduced to a great extent, some may still persist, particularly in continuously cloudy areas. These features are likely to result in a spatial variability in albedo which in turn could result in incorrectly classified slush-pixels.

4.3.2 Classification

In the classification there is one main flaw in its way of classifying slush. This flaw refers to the fact that potential slush cells include neighboring land or water pixels in calculating the spatial variability of albedo. Due to the very different spectral properties of land and water compared to what is on the ice, it is very likely that this inclusion results in a high spatial variability of albedo. Because of that, cells with neighboring land or water cells are likely to be classified as slush due to a spatial variability that in reality is not attributed to slush or within what is on the ice. An example of this type of misclassification is seen in Figure 2.

This flaw is partly dealt with as it often incorrectly detects slush-pixels regardless of season which therefore puts the pixel above the threshold of cumulative slush-days and consequently do not classify it as slush. However, there may still be some pixels that are incorrectly classified. In Figure 11b, it is seen that one slush pixel is detected in the Northwestern corner. That pixel has 7 neighboring land cells and one that is considered on top of ice. Here, it is classified as slush because of a spatial variability based on the variability of albedo between land pixels and the two lone ice pixels. This does not agree with the theory of slush being an area of higher spatial variability in albedo *on* the ice sheet. From the visual interpretation of a satellite image, no slush is identified in that area.

In order to improve the classification, the neighboring cells should be considered only if they are on the ice. A spatial variability of albedo should be based solely on what is on the ice, as limits between ice and land or ice and water expect to increase the spatial variability.

Using limits in absolute values of albedo in order to distinguish slush-pixels from other pixels is a method that perhaps could be used if there were information on absolute albedo values of slush. However, slush can vary greatly in terms of albedo and the albedo-values between which it can range are different depending on location and climate. It is therefore hard to find a global threshold which can represent the whole GrIS and correctly classify slush-pixels in very different areas based on absolute values of albedo.

A different potential source of misclassification could be crevasses in the ice. With the movement of ice comes the formation of crevasses which can be described as a deep crack in the ice. These could be several hundred meters long but typically have a width of less than 20 m. This does not nearly cover an entire cell in our albedo grids but could play a role in altering the albedo as it is a notably darker element in the area. Areas with many crevasses could therefore have a higher spatial variability due to the presence of crevasses, and not slush.

For future work, an improved classification should include consideration of neighboring cells only if they are lying on top of ice. This would correctly produce results where slush is defined by the spatial variability between surfaces on ice. Additionally, a threshold value should be set using several sources of information. High-resolution satellite imagery in which slush can be observed is one suggestion. Another one is to use multiple specific locations where a slush-line has been observed. With locations of the slush-line considered as ground-truth, as well as high resolution satellite imagery containing information on slush, a classification using different threshold values can be tested and compared with the ground-truth.

This way a threshold value which is more representable for the whole ice sheet and produces results that agree with several points of ground-truth can be set to classify the GrIS.

4.4 Discussion of analysis and validation

4.4.1 Preliminary sensitivity analysis
Looking at the GrIS as a whole, it seems from a visual analysis that western areas were the most sensitive to a changed threshold value. Quantitative analysis of the changes indicates that western areas indeed are the most sensitive. Figure 10 shows that if drainage basin 2.1 is disregarded, no drainage system is more sensitive than the western ones of 6.1, 6.2, 7.1, 7.2 and 8.1. This is interesting as they all belong to those that are described as most suitable for slush-extent and slush-line analysis in this study.

An important outtake from the threshold comparison is the sensitivity of drainage system 6.2. This drainage system showed the greatest sensitivity of all when the threshold was changed from a standard deviation of 4 % to that of 5 %. Going from 5 to 6 %, it was the second most sensitive. Drainage system 6.2 is also where KAN_U automatic weather station is found. That means that the classification was adapted to a ground-truth which is based on a location in the most sensitive drainage system. Essentially, there is no area where it is more crucial to get a correct value of threshold. It is in drainage system 6.2 that a changed threshold causes the biggest difference. Although drainage systems are large, this provides some confidence as our threshold value is fitted specifically to recreate the ground-truth of an area belonging to the most sensitive across the ice sheet.

4.4.2 Visual validation
A visual validation gives an impression that the classification works in the sense that it gives an output that seems realistic. A comparison indicates that the classified image shows a similar pattern compared to satellite image. At the very margin of the ice sheet, by land areas we can see that there is bare ice both in the satellite image and the classification. Eastward, the area transitions to one of slush. Further east, there is no slush but dry snow. Generally, these patterns are found both in the interpreted satellite image and the classified image. The classification is not completely accurate and shows some slush present in an area that in reality is bare ice, and there are definitely some errors. The coarser resolution also proves the lack of detail when the classified image is compared to the interpreted satellite image.

The validation is purely visual but is used to give an impression on whether or not our classification can be considered realistic. The satellite image used is from western Greenland and the classification displayed therefore belongs to the more reliable detections of slush. It should be noted that only one satellite image from a single day and one area is being used. In order to perform a more extensive validation to add more confidence to the classification a similar validation needs to be made for more days and areas of Greenland.

5. Conclusion
In this study, the spatial variability in albedo in satellite data was used to study the spatiotemporal behavior of slush. Over the study period 2000–2019 slush was successfully detected using coarse resolution satellite imagery. Results indicate fluctuations in quantity of slush which reached a substantial

peak in the summer of 2012. A median slush-extent was calculated to be 587 350 km$_2$ and a median slush-line elevation was 1888 meters above sea-level. The development generally follows a pattern that is similar to the estimated surface mass balance patterns described in previous studies. In particular, the patterns of slush-extent calculated agrees quite well with patterns of measured melt-extents from NSIDC. Slush-areas were only found in association with the melting season on Greenland.

A spatial pattern was observed where most slush is found on the western areas of the ice sheet, some is found in the north and little is found on the eastern parts of the ice sheet. Because of the spatial distribution of slush and a more complex topography in the east, the western and southern drainage basins show more of an agreement between the development of slush-extent and slush-line elevation. Here, correlation coefficients range between 0.446 and 0.821. In those areas, the slush-line migrates to higher elevations together with an increased slush-extent. The difficulties in finding representable results in the east as well as the fact that the classification is both evaluated in the west and adapted to an area in the west make western areas more suitable for study and detection of slush using our methodology.

Future work on this topic can be made in order to create more accurate classifications which could detect slush on the GrIS. An extensive method using multiple ground-truth points should be used in order to set a threshold value for spatial variability in albedo with great confidence. These ground-truth points should be widespread across different locations on the ice sheet to create a globally applicable threshold value. If future work could use satellite data of higher spatial resolution as well as considering only cells on ice when calculating spatial variability in albedo, it has the potential to detect slush with a high accuracy.

References

Bamber, J. L., R. M. Westaway, B. Marzeion, and B. Wouters. 2018. The land ice contribution to sea level during the satellite era. *Environmental Research Letters,* 13. DOI: 10.1088/1748-9326/aac2f0

Boggild, C. E., R. E. Brandt, K. J. Brown, and S. G. Warren. 2010. The ablation zone in northeast Greenland: ice types, albedos and impurities. *Journal of Glaciology,* 56**:** 101-113. DOI: 10.3189/002214310791190776

Box, J. E., X. Fettweis, J. C. Stroeve, M. Tedesco, D. K. Hall, and K. Steffen. 2012. Greenland ice sheet albedo feedback: thermodynamics and atmospheric drivers. *Cryosphere,* 6**:** 821-839. DOI: 10.5194/tc-6-821-2012

Box, J. E., van As, D., Steffen, K., Fausto, R. S., Ahlstrøm, A. P., Citterio, M., Andersen, S. B. 2017. MODIS Greenland albedo.

Ewert, H., A. Groh, and R. Dietrich. 2012. Volume and mass changes of the Greenland ice sheet inferred from ICESat and GRACE. *Journal of Geodynamics,* 59**:** 111-123. DOI: 10.1016/j.jog.2011.06.003

Greuell, W., and W. H. Knap. 2000. Remote sensing of the albedo and detection of the slush line on the Greenland ice sheet. *Journal of Geophysical Research-Atmospheres,* 105**:** 15567-15576. DOI: 10.1029/1999jd901162

Hofer, S., A. J. Tedstone, X. Fettweis, and J. L. Bamber. 2017. Decreasing cloud cover drives the recent mass loss on the Greenland Ice Sheet. *Science Advances,* 3. DOI: 10.1126/sciadv.1700584

IMBIE Team 2020. Mass balance of the Greenland Ice Sheet from 1992 to 2018. *Nature,* 579**:** 233-+. DOI: 10.1038/s41586-019-1855-2

IPCC, 2014. Climate Change 2014: Synthesis Report. Contribution of Working Groups I, II and III to the Fifth Assessment Report of the Intergovernmental Panel on Climate Change. IPCC, Report, Geneva, Switzerland. [in Swedish, English summary]

Knap, W. H., and J. Oerlemans. 1996. The surface albedo of the Greenland ice sheet: Satellite-derived and in situ measurements in the Sondre Stromfjord area during the 1991 melt season. *Journal of Glaciology,* 42**:** 364-374. DOI: 10.3189/s0022143000004214

Lacour, A., H. Chepfer, N. B. Miller, M. D. Shupe, V. Noel, X. Fettweis, H. Gallee, J. E. Kay, et al. 2018. How Well Are Clouds Simulated over Greenland in Climate Models? Consequences for the Surface Cloud Radiative Effect over the Ice Sheet. *Journal of Climate,* 31**:** 9293-9312. DOI: 10.1175/jcli-d-18-0023.1

Mikkelsen, A. B., A. Hubbard, M. MacFerrin, J. E. Box, S. H. Doyle, A. Fitzpatrick, B. Hasholt, H. L. Bailey, et al. 2016. Extraordinary runoff from the Greenland ice sheet in 2012 amplified by hypsometry and depleted firn retention. *Cryosphere,* 10**:** 1147-1159. DOI: 10.5194/tc-10-1147-2016

Neumann, B., A. T. Vafeidis, J. Zimmermann, and R. J. Nicholls. 2015. Future Coastal Population Growth and Exposure to Sea-Level Rise and Coastal Flooding - A Global Assessment. *Plos One,* 10. DOI: 10.1371/journal.pone.0118571

Nghiem, S. V., D. K. Hall, T. L. Mote, M. Tedesco, M. R. Albert, K. Keegan, C. A. Shuman, N. E. DiGirolamo, et al. 2012. The extreme melt across the Greenland ice sheet in 2012. *Geophysical Research Letters,* 39. DOI: 10.1029/2012gl053611

Nicholls, R. J., N. Marinova, J. A. Lowe, S. Brown, P. Vellinga, D. De Gusmao, J. Hinkel, and R. S. J. Tol. 2011. Sea-level rise and its possible impacts given a 'beyond 4 degrees C world' in the twenty-first century. *Philosophical Transactions of the Royal Society a-Mathematical Physical and Engineering Sciences,* 369**:** 161-181. DOI: 10.1098/rsta.2010.0291

NSIDC. 2019. Greenland Ice Sheet Melt Characteristics Derived from Passive Microwave Data, Version 1.

Rignot, E. I. V., M. R. van den Broeke, A. Monaghan, and J.T.M. Lenaerts. 2011. Acceleration of the contribution of the Greenland and Antarctic ice sheets to sea level rise. *Geophysical Research Letters,* 38. DOI: 10.1029/2011GL046583

Ryan, J. C., L. C. Smith, D. van As, S. W. Cooley, M. G. Cooper, L. H. Pitcher, and A. Hubbard. 2019. Greenland Ice Sheet surface melt amplified by snowline migration and bare ice exposure. *Science Advances,* 5. DOI: 10.1126/sciadv.aav3738

Scambos, T., Stroeve, J., Koenig, L. 2019. Greenland Ice Sheet Today | Surface Melt Data presented by NSIDC. Retrieved 2020-04-10 2020, from http://nsidc.org/greenland-today/.

Sharpnack, D. A., and G. Akin. 1969. AN ALGORITHM FOR COMPUTING SLOPE AND ASPECT FROM ELEVATIONS. *Photogrammetric Engineering,* 35**:** 247-+.

Sinergise Ltd. 2020. Modified Copernicus Sentinel Data. ed. S. Hub. Ljubljana, Slovenia.

Stephens, G. L., J. M. Slingo, E. Rignot, J. T. Reager, M. Z. Hakuba, P. J. Durack, J. Worden, and R. Rocca. 2020. Earth's water reservoirs in a changing climate. *Proceedings of the Royal Society a-Mathematical Physical and Engineering Sciences,* 476. DOI: 10.1098/rspa.2019.0458

van den Broeke, M., P. Smeets, J. Ettema, C. van der Veen, R. van de Wal, and J. Oerlemans. 2008. Partitioning of melt energy and meltwater fluxes in the ablation zone of the west Greenland ice sheet. *Cryosphere,* 2**:** 179-189. DOI: 10.5194/tc-2-179-2008

van den Broeke, M. R., E. M. Enderlin, I. M. Howat, P. K. Munneke, B. P. Y. Noel, W. J. van de Berg, E. van Meijgaard, and B. Wouters. 2016. On the recent contribution of the Greenland ice sheet to sea level change. *Cryosphere,* 10**:** 1933-1946. DOI: 10.5194/tc-10-1933-2016

Vaughan, D. G., J.C. Comiso, I. Allison, J. Carrasco, G. Kaser, R. Kwok, P. Mote, T. Murray, F. Paul, J. Ren, E. Rignot, O. Solomina, K. Steffen, T. Zhang, 2013. Observations: Cryosphere. Report 317-382 pp.

Velicogna, I. 2009. Increasing rates of ice mass loss from the Greenland and Antarctic ice sheets revealed by GRACE. *Geophysical Research Letters,* 36. DOI: 10.1029/2009gl040222

Zwally, H. J., Giovinetto, M. B., Beckley, M. A., Saba, J. L. 2012. Antarctic and Greenland Drainage Systems. ed. G. C. S. Laboratory.
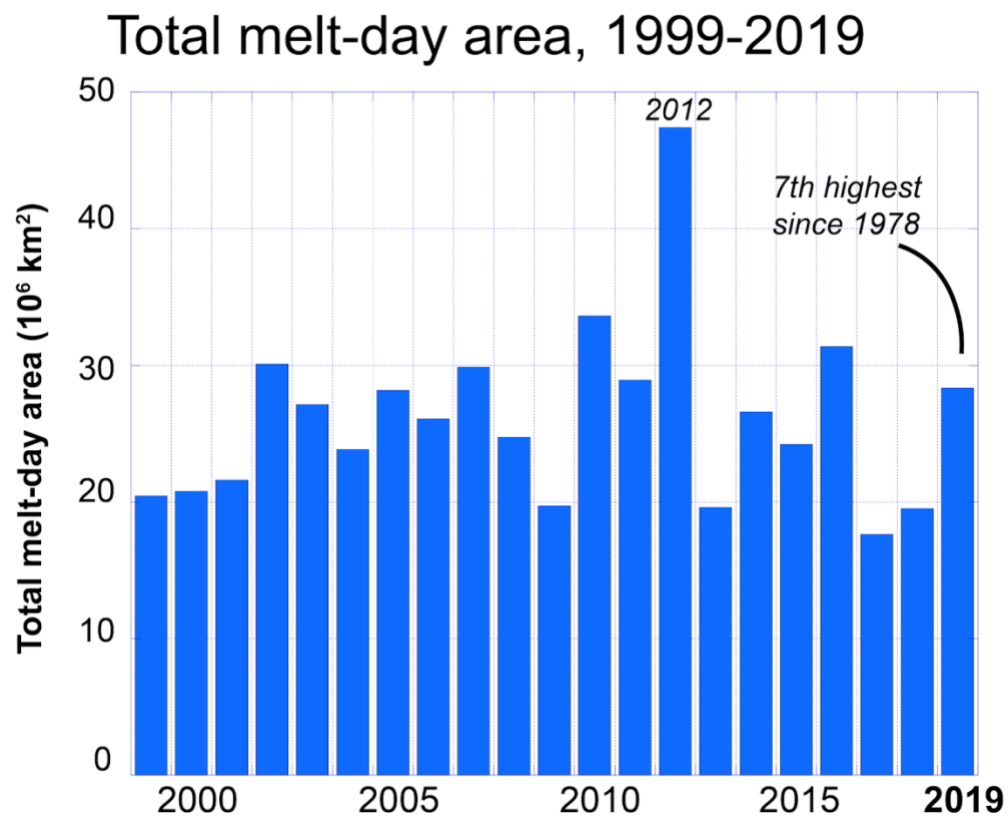
Appendix A

Total melt-day area, 1999-2019

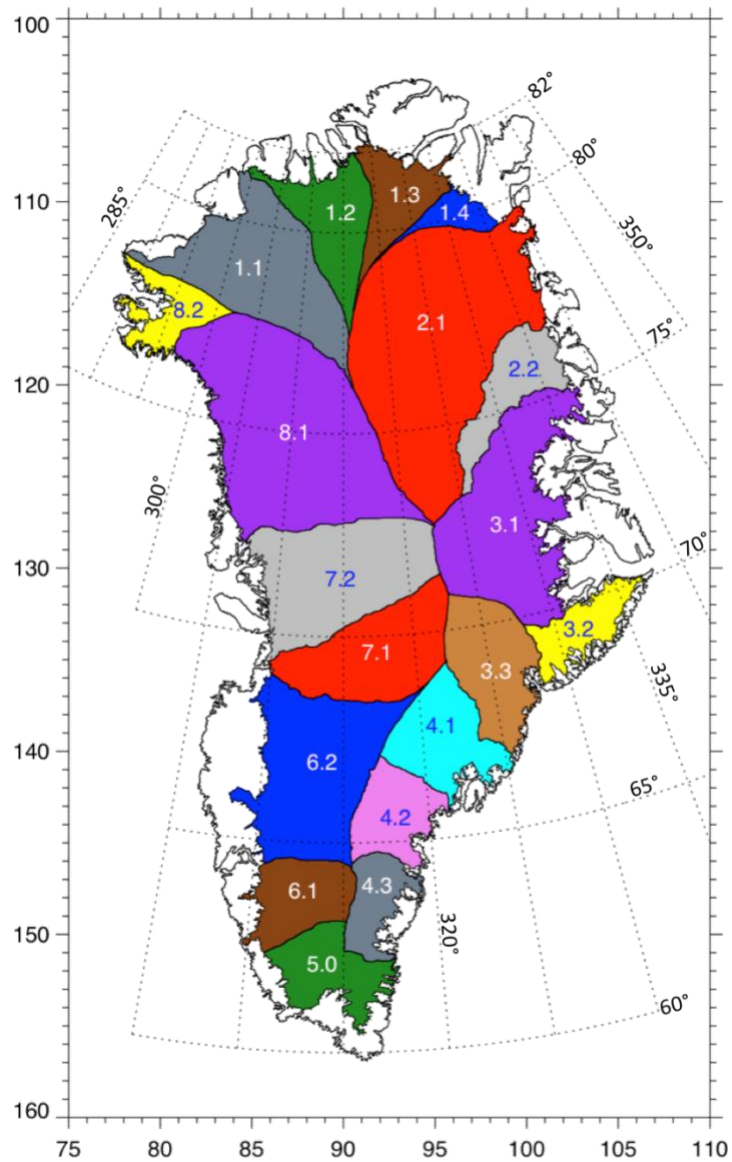**Figure A1: Melt-extents in cumulative melt-day area, Source: NSIDC**

Figure A2: Drainage systems of Greenland, Source: Zwally (2012) (NASA)